University of British Columbia

Social Ecological Economic Development Studies (SEEDS) Sustainability Program

Student Research Report

Assessing the Effect of Tree Stand Composition on Urban Cooling Effect on the UBC Vancouver Campus

Prepared by: Zitong Xu

Prepared for: UBC Campus + Community Planning

Course Code: FCOR 599

University of British Columbia

Date: 8 April 2023

Assessing the Effect of Tree Stand Composition on Urban Cooling Effect on the UBC Vancouver Campus Using the 2021 Western North America Heat Wave

Zitong Xu, BSc

The University of British Columbia

FCOR 599: Final Research Report

Topical Mentor: Emma Luker, UBC Campus + Community Planning

April 8th, 2023

Abstract

Rapid urbanization leads to the reduction of urban greenspaces, affecting the urban thermal environment and exacerbating the urban heat island effect. As urban forests are effective contributors to mitigating the urban heat island effect, understanding the composition of urban forests is important for assessing cooling effects. In response to growing concerns about the urban heat island effect, recent studies have used satellite imagery to investigate the cooling effects of urban forests' characteristics, as remotely sensed data are flexible in spatial and temporal resolutions. This study determined the spatial patterns of land surface temperatures and tree stand compositions, as well as examined the cooling effects of different tree stand compositions at the UBC Vancouver campus during the 2021 Western North America Heat Wave. This study was done by retrieving land surface temperatures from Landsat 8 images and using grid-based analysis to classify tree stand composition in the following classification schemes: coniferous, deciduous, and mixed wood. A linear mixed effects model was also conducted to quantify the relationship between land surface temperature differences and tree stand compositions throughout the Heat Wave. The results showed that coniferous stand composition was positively correlated, but deciduous stand composition was negatively correlated with land surface temperature differences. The findings indicated that expanding forested areas could lower land surface temperatures, and deciduous stand composition has the greatest cooling effectiveness. Overall, this study would provide valuable insights for UBC campus planners seeking to implement new strategies to enhance the resilience of the campus climate.

Keywords: Land Surface Temperatures, Urban Heat Island Effect, Urban Forestry, Tree Stand Composition, 2021 Western North America Heat Wave, UBC

Table of Contents

1. Introduction

1.1 Contribution of Urban Forests to Urban Cooling

With the acceleration of global urbanization, the expansion of urban areas is characterized by converting natural surfaces to artificial impervious surfaces (Zuo et al., 2018). Urban sprawl reduces the number of urban greenspaces and increases heat emissions, which consequently causes excessive heat storage on urban surfaces (Aminipouri et al., 2019). The lack of restrictive policies for urban sprawl and poorly planned urban development are also exacerbating urban greenspaces reduction and Urban Heat Island effect (Naeem et al., 2018). Urban Heat Island (UHI) effect refers to a phenomenon that urban cores are warmer than their surrounding rural areas (Jiao et al., 2017). The resulting increased land surface temperatures (LST) from the UHI effect lead to decreased thermal comfort for citizens and increased energy consumption for cooling indoor environments (e.g., air conditioning) (Zhou et al., 2019). These effects also significantly increase air pollutants (Zhao et al., 2020), exacerbate the energy crisis, and raise heat-related mortality (e.g., heat exhaustion and heat stroke) (Aminipouri et al., 2019). As the urban forests are one of the effective ways to reduce LST in urban areas, it is important to understand the contribution of urban forests to mitigate UHI effects.

Urban forests as an influential contributor to mitigating the UHI effect, especially during the summer, providing shaded areas and absorbing thermal radiation through transpiration and evaporation (Naeem et al., 2018). Several studies investigated the cooling effects of urban forests' characteristics (Wang et al., 2018), canopy characteristics (Richter et al., 2021), and patch size of greenspace (Jiao et al., 2017) on LST in different cities. Differences in planting configuration and characteristics of tree species can influence the ability of urban forests to reduce LST, depending on physiological and meteorological properties of trees, such as transpiration rates, crown size, and crown density (Richter et al., 2021; Zhao et al., 2020). Eyster & Beckage (2022) also discovered that the cooling effect of urban forests could vary by four times from species to species due to differences in shading capacity and transpiration rates. As the broadleaf tree has a higher albedo and a lower transpiration rate, it reduces LST more efficiently than conifers in Europe (Schwaab et al., 2020). In addition, increasing urban forests not only can mitigate the UHI effect, but also increase humidity and reduces dust in urban areas

(Jiao et al., 2017). Thus, the ability of urban forests to alter LST needs to be assessed to inform the development of adaptive urban planning strategies to mitigate the impact of UHI effectively. However, the relationship between tree stand compositions and LST on a finer scale and the optimal tree stand composition that can effectively cool urban areas have been poorly studied.

As sensor design continues to improve and data processing algorithms are developed, various remote sensing (RS) data and GIS techniques are more widely used to retrieve LST (Wang et al., 2019). RS data are generally publicly available and can be used for large-scale analysis of the relationships between LST and other environmental factors (Richter et al., 2021), such as canopy size, land cover, and vegetation cover. RS data are also flexible in spatial and temporal resolutions (Wang et al., 2019), making it easier to spatially compare the cooling effects of urban forests. Thus, previous studies regarding LST mainly derived LST from the thermal infrared band of satellite imagery (Hou & Estoque, 2020; Zhou et al., 2019). Additionally, Eyster and Beckage (2022) used LST derived from Landsat images to explore the impact of trees and land cover on LST. In this study, I derived LST from the Landsat 8 images, offering a more efficient and accurate approach to retrieving and analysing LST.

1.2 Western North America Heat Wave in 2021

Although Western Canada historically has not been commonly subject to extreme heat (Stewart et al., 2017), Western North America Heat Wave hit this region in the summer of 2021. Particularly, this heat wave broke the air temperature record in Vancouver, British Columbia (Eyster & Beckage, 2022), which consequently influenced LST on the University of British Columbia Vancouver (UBCV) campus. This heat wave lasted from June 24 to July 7, 2021, and LST warmed up to 30.4 °C (Cotlier & Jimenez, 2022), influencing natural and residential neighborhoods' living environments on the UBCV campus. To improve the thermal comfort conditions across the UBCV campus, it is crucial to assess the planting composition of urban forests to inform campus planners how to minimize the impact of extreme heat using optimal tree stand composition. Additionally, the effects of tree stand compositions under extreme hot weather remains uncertain. Therefore, assessing the impact of tree stand compositions could be a valuable contribution to improving UBC's climate resilience while guiding the decision-making process for developing Campus Vision 2050 (Campus Version 2050, n.d.).

1.3 Research Objectives

To enhance understanding of the cooling effects of urban forests on a finer scale, this study investigated the effect of three tree stand compositions on the LST during the 2021 Western North America Heat Wave ("the Heat Wave") on the UBCV campus. The objectives of this study were 1) determine the spatial pattern of LST on the UBCV campus; 2) classify tree stand composition within the UBCV campus in the following classification scheme: coniferous, deciduous, and mixed wood stand compositions; 3) assess the cooling impact of each tree stand composition on LST throughout the Heat Wave; 4) determine the optimal tree stand composition that most effectively mitigates LST. The findings informed how different tree species compositions affect the cooling effects and enhance the understanding of the effect of the spatial configuration of trees on the cooling effectiveness. Overall, the conclusions drawn by this study contributed to urban forest management and policies on the UBCV campus related to creating resilient and climate-adapted ecosystems on campus.

2. Study Area and Data Description

2.1 Study Area: UBC Vancouver Campus

The University of British Columbia Vancouver (UBCV) campus, also known as the Point Grey campus, is located at the western tip of the Point Grey Peninsula in Vancouver, British Columbia, Canada (49.2606° N, 123.2460° W) (Figure 1) (UBC Campus & Community Planning, n.d.). The UBCV campus is surrounded by dense forest and ocean with gentle topography, and covers more than 400 hectares (UBC Campus & Community Planning, n.d.). As the UBCV campus is entirely within the Coastal Western Hemlock Biogeoclimatic Zone (CWH) (BEC WEB, n.d.), suitable for temperate mixed woods, resulting in a higher diversity of the tree species on the campus. According to the Tree Inventory Project reported by the UBC Social Ecological Economic Development Studies (SEEDS) Program, the UBCV campus is dominantly surrounded by western red cedar, red alder, Douglas fir, black cherry, and Norway maple (Devisscher & Almas, 2020). The UBCV campus has also planted approximately 8,000 trees since 1925 (Sutherland, 2012). Additionally, the UBCV campus has a moderate oceanic climate that borders on the mild dry summer and wet winter (Gülçin et al., 2021). However, the UBCV campus expanded its urban coverage of buildings, roads, and neighborhood housing communities since the early 20th century. Due to the campus expansion and fuel woods harvesting, 24% of the canopy cover on the UBCV campus declined in recent years, especially conifer cover (Sutherland, 2012). Therefore, the UBCV campus can provide detailed information on the composition of the current status of urban forests, which is an important area for quantifying and assessing urban forest management on a finer scale.

Figure 1. Legal boundary of the University of British Columbia Vancouver (UBCV) campus. The UBCV campus is composed with dense trees and urban forests. The inset shows the location of the UBCV campus in the Metro Vancouver. The bases map is projected in NAD 1983 UTM Zone 10N and sourced from ESRI. Data is sourced from the University of British Columbia Campus and Community Planning (2013).

2.2 Data Description

This study used campus and community planning data, soft landscape data, campus tree data, and three Landsat 8 images (Table 1). A detailed data description of each dataset is described in the section below.

Table 1. Overview of dataset name, file type, source, and access of each dataset were used for conducting this study.

	Dataset name	File Type	Source	Access
Campus and Community Planning Data	LegalBoundaryL	Shapefile	https://hdl.handle.net/11272.1/AB2/ETO8IU	Public
Campus Tree Data	ubcv_campus_trees	CSV file	https://github.com/UBCGeodata/ubc-geospatial-opendata/tree/master/ubcv/landscape	Public
Soft Landscape Data	Soft_landscape	GeoJSON	https://github.com/UBCGeodata/ubc-geospatial-opendata/tree/master/ubcv/landscape	Public
Landsat 8 OLI/TIRS Collection 2 Level-1 Science Products	See Table 2 for details	Raster	https://earthexplorer.usgs.gov	Public

2.2.1 Campus and Community Planning Data

Campus and Community Planning data is an Esri ArcGIS geodatabase with the UBCV campus spatial data. It is freely available for downloading on the Abacus Data Network (The University of British Columbia Campus and Community Planning, 2013). This geodatabase consists of various shapefile datasets, including buildings base data, campus-related data, legal boundary, and UBC Mobile data. The legal boundary of the UBCV campus was exported from this geodatabase and sever as the shapefile (line feature) for the project boundary (Figure 1). The projected coordinate system of the UBC legal boundary is NAD 1983 UTM Zone 10N.

2.2.2 Campus Tree Data

Campus tree data contains spatial and species information on current campus trees (7000 observations for 180 distinct tree species). This data was published in 2013, but is continually updated based on field observations. Based on its metadata, tree locations were derived and identified from the 2019 orthophoto, species ID was created by Egan Davis, tree measurements were taken by students from UFOR101 class, and tree heights were derived from 2018 Lidar (UBCGeodata, n.d.). Campus tree data is also publicly available and was downloaded online via the UBCGeodata (UBCGeodata, n.d.). This data is a CSV file that need to be converted to a new point feature class ("campus trees"), to further identify tree stand compositions on the UBCV campus.

2.2.3 Soft Landscape Data

Soft landscape data includes spatial information on the lawn, planting bed, planting bed on structure, athletic field, and wild areas of the soft landscape. This data was derived from UBCGeodata and is publicly available on GitHub (UBCGeodata, n.d.). Soft landscape data is GeoJSON data, projected in WGS84. Each green space had an associated green space planting bed ID. As wild areas of soft landscape indicate the urban forests on the UBCV campus, a new polygon feature class ("urban forests") was identified and extracted from this dataset. The new feature class was used to visually analyze the relationship between urban forests and LST.

2.2.4 Landsat 8 OLI/TIRS Collection 2 Level-1 Science Products

Landsat 8 OLI/TIRS Collection 2 Level-1 science products were acquired from the Landsat 8 OLI/TIRS sensor and downloaded from the U.S. Geological Survey (Earth Explore, n.d.). To minimize the classification error caused by clouds, "Less than 30%" Scene Cloud Cover were included as additional criteria for filtering satellite imagery. According to the Vancouver Historical Temperature (n.d.), the air temperature records in Vancouver were broken on June 24th, 2021. Therefore, three Landsat 8 images were used to indicate the LST before, during, and after the Heat Wave (Table 2). The thermal infrared band (Band 10) of these images can be used to derive LST and explore the spatial pattern of LST on the UBCV campus.

Table 2. Overview of three Landsat 8 images information.

	LC08_L1TP_047026_20210529_20210608_02_T1	**LC08_L1TP_047026_20210630_20210708_02_T1**	**LC08_L1TP_047026_20210902_20210910_02_T1**
Acquisition date	2021/05/29	2021/06/30	2021/09/02
Land cloud cover (%)	1.48	23.30	1.89
Sensor	Landsat 8 OLI/TIRS		
Spatial resolution	Band 10: 100 m		
Spectral resolution	11 Bands		
Temporal resolution	16 days		
Radiometric resolution	12 bits		

3. Methods

To analyze the cooling effect of three tree stand compositions on LST on the UBCV campus during the Heat Wave, this study was done by 1) retrieving LST, 2) identifying tree stand compositions, and 3) statistical analyzing the relationship between ΔLST and tree stand compositions at two different time points. Data processing was conducted in ArcGIS Pro v. 2.8.6 (Esri Inc., 2022), and statistical analysis was performed in RStudio 2023.03.0+386 (RStudio Team., 2020). A workflow diagram for the methodology is presented in Figure 3.

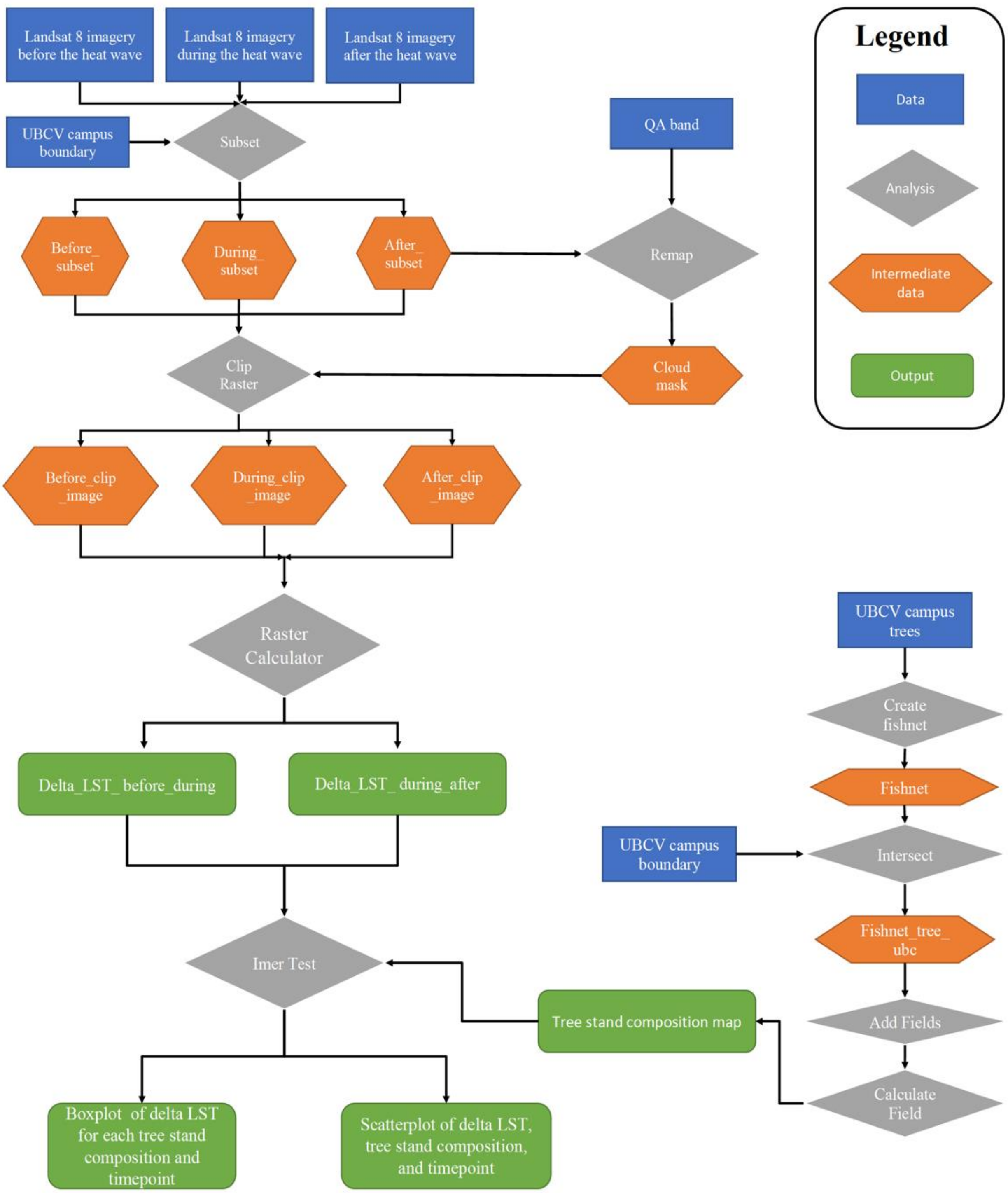

Figure 3. Workflow diagram of analysis for understanding how tree stand composition affects their cooling effectiveness on the UBCV campus throughout the Heat Wave. The process can be divided into land surface temperature retrieval, tree stand composition identification, and statistical analysis.

3.1 Land Surface Temperature (LST) Retrieval

3.1.1 Data Pre-processing

To retrieve the LST from the thermal infrared (TIR) band of Landsat 8 OLI/TIRS Collection 2 Level-1 products, I chose three satellite images that were taken in late May, late June, and early September, to respectively represent the LST before, during, and after the Heat Wave. Extreme hot weather started from late June through mid-July 2021 (Cotlier & Jimenez, 2022), and these images can therefore capture changes in LST throughout the Heat Wave. These satellite images were then subsetted by the legal boundary of the UBCV campus to reduce the computational processing load. To remove cloud and shadow from these satellite images, I created a cloud mask by filtering QA pixels with values 21824 and 21925, since these values correspond to clear terrain and water, while all other values are clouds and shadows (Lenhardt, n.d.; U.S. Geological Survey, n.d.).

3.1.2 Calculation of LST Difference

To determine the spatial variation of LST on the UBCV campus, I calculated the LST differences (ΔLST) between before and during the Heat Wave (before ~ during), as well as, between during and after the Heat Wave (during ~ after). Landsat 8 TIR band (Band 10) can be used for LST calculation because it provides metadata of the bands, such as thermal constant and rescaling factor values (Jesus & Santana, 2017). According to the equation provided by Rosado et al. (2020), a flowchart for calculating ΔLST is shown in Figure 4.

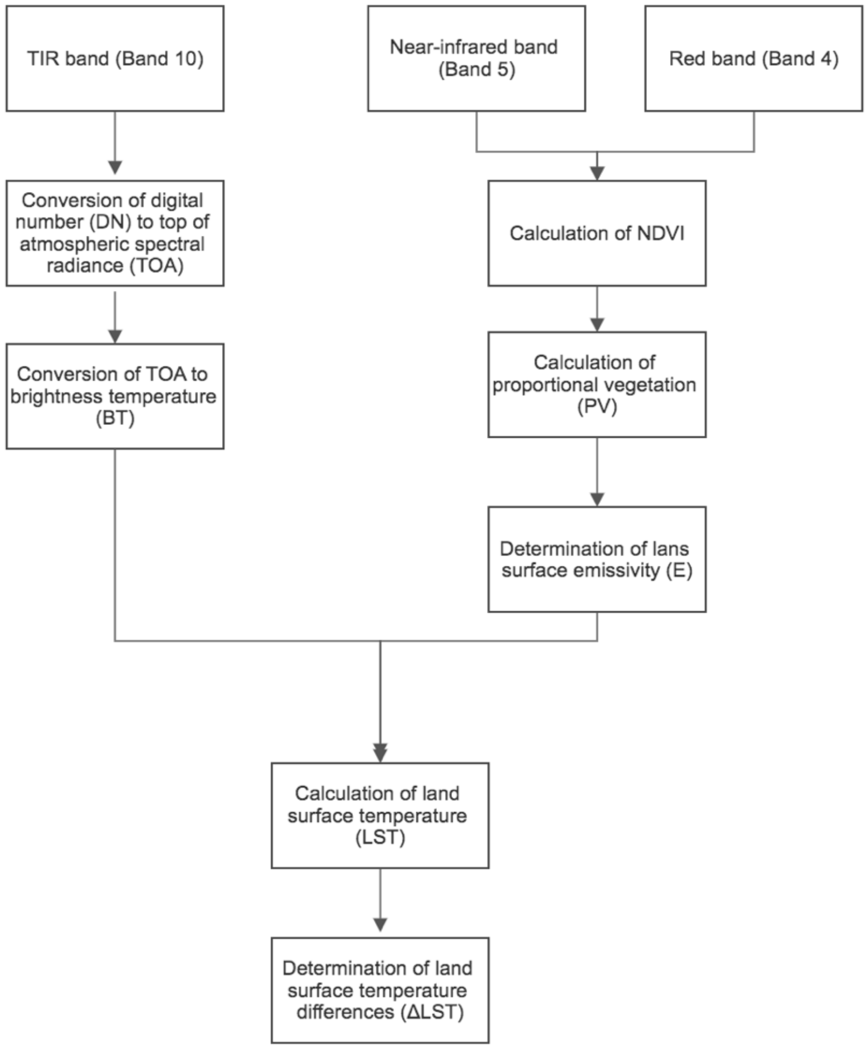

Figure 4. Flowchart for calculating land surface temperature differences (ΔLST).

To perform the conversion of the digital number values of each pixel to spectral radiance, the Top of Atmospheric (TOA) spectral radiance was first calculated by multiplying the corresponding Band 10 with a multiplicative rescaling factor (M_L) and adding the additive rescaling factor (A_L) (Table 3, Equation 1). TOA was then converted to top of atmosphere brightness temperature (BT) by computing two band-specific thermal conversion constants (Table 3, Equation 2), because BT is independent of atmospheric conditions that allows for more accurate comparisons of thermal information from different times (Rosado et al., 2020). As land surface emissivity (E) affects the amount of thermal radiation emitted by the Earth's surface (GIS-Blog., n.d.), I then calculated E (Table 3, Equation 5), which was computed from NDVI values (Table 3, Equation 3) and the proportion of vegetation (Table 3, Equation 4).

To determine the change in LST throughout the Heat Wave, LST in degrees Celsius was calculated using BT, E, and the wavelength of the emitted radiation (Table 3, Equation 6). Three raster layers (LST before, during, and after the Heat Wave) were then generated, and each pixel contained a single value representing LST. Finally, I subtracted LST before from LST during, and LST during from LST after to generate two ΔLSTs (before ~ during, and during ~ after) for later statistical analysis.

Table 3. Overview of all equations used to calculate LST, including the name, units, and formula of the equations, as well as, the values and descriptions of the fundamental constants involved in the equations. All equations are provided by Rosado et al. (2020).

	Name	Units	Formula	Fundamental Constants	Description of Fundamental Constants
Equation 1	Top of Atmospheric spectral radiance	Watts/(m²*srad*µm)	$TOA = M_L Q_{cal} + A_L$	$M_L = 3.342e-04$ Qcal = 3.3420e-04 $A_L = 0.1$	M_L: Specific multiplicative scaling factor of each band Q_{cal}: Reflectance of band 10 A_L: Additive rescaling factor
Equation 2	Top of atmosphere brightness temperature	Degree Celsius (°C)	$BT = \frac{K_2}{In(\frac{K_1}{TOA}+1)} - 273.15$	$K_1 = 774.8853$ $K_2 = 1321.0789$	K_1: Conversion constants, included in the metadata K_2: Conversion constants, included in the metadata
Equation 3	Normalized difference vegetation index	N/A	$NDVI = \frac{NIR - RED}{NIR + RED}$	N/A	N/A
Equation 4	Proportion of vegetation	N/A	$P_v = (\frac{NDVI - NDVI_{min}}{NDVI_{max} - NDVI_{min}})^2$	N/A	N/A
Equation 5	Land surface emissivity	N/A	$E = 0.004 \times P_v + 0.986$	N/A	N/A
Equation 6	Land surface temperature	Degree Celsius (°C)	$LST = \frac{BT}{1 + \left(\frac{10.8 \times BT}{14380}\right) \times lnE}$	N/A	N/A

3.2 Tree Stand Compositions Identification

To examine the influence of tree stand compositions on LST, I applied a grid-based analysis using polygon grids (Hou & Estoque, 2020). A new polygon layer with rectangular grids, also known as a fishnet, was created with a 30m cell width and height because the cell size of the fishnet needs to match the spatial resolution of the Landsat 8 TIR band. The fishnet layer was then intersected by the legal boundary of the UBCV campus to ensure the fishnet fits within the study area.

To identify the tree stand composition on the UBCV campus, the attribute table of campus tree data was re-arranged because all Null values from the genus column need to be removed. Three new fields were added to the attribute table of the new polygon features of trees, including the total number of trees, percent of deciduous, and tree stand composition class (Table 4). Meanwhile, the values of these new fields for each grid were calculated based on the definition (Table 4) (Eyster & Beckage, 2022).

Table 4. Overview of three new fields were added to the attribute table of new polygon features of trees.

	Definition	Field Name	Type
Total number of trees	Total number of trees occur within each grid cell	total_trees	Double
Percent of deciduous	Percentage of deciduous trees within each grid cell.	%_deciduous	Float
Tree stand composition class	• 0% -35% deciduous: coniferous stand composition • 35% -75% deciduous: mixed wood composition • 75%-100% deciduous: deciduous stand composition	class_composition	Float

3.3 Statistical Analysis

A linear mixed effects model was conducted to quantify the relationship between ΔLST and tree stand compositions at two different time points (before ~ during, and during ~ after), where tree stand composition is the factor variable, ΔLST is the dependent variable, and time point is the class variable. The model involved variance across two time points because the ΔLST varies by time and affects the correlation between tree stand composition and ΔLST. I also performed the F-test to test whether the mean ΔLST significantly differs among three tree stand compositions. As I have found differences, I continued to examine which pair of tree stand composition significantly differ from each other using Bonferroni adjustment, the pairs of means t-tests. Based on the statistical results, I can finally analyze the model performance for each tree stand composition and interpret the impact of tree stand composition on cooling effect.

4. Results

4.1 Spatial Pattern of LST Differences

To explore the spatial variation of the ΔLST on the UBCV campus during the Heat Wave, Figure 5 showed the spatial distribution of two ΔLSTs (before ~ during and during ~ after). Between before and during the Heat Wave (Figure 5, left), ΔLST ranged from the lowest point of -0.193 °C shown in dark blue to the highest point of 6.099 °C shown in dark red. ΔLST between during and after the Heat Wave (Figure 5, right) ranged from -4.555°C to -0.462°C . The spatial patterns of the two ΔLSTs were consistent that the center of the campus had lower change in LST, while ΔLST was higher at the edge of the campus throughout the heat wave.

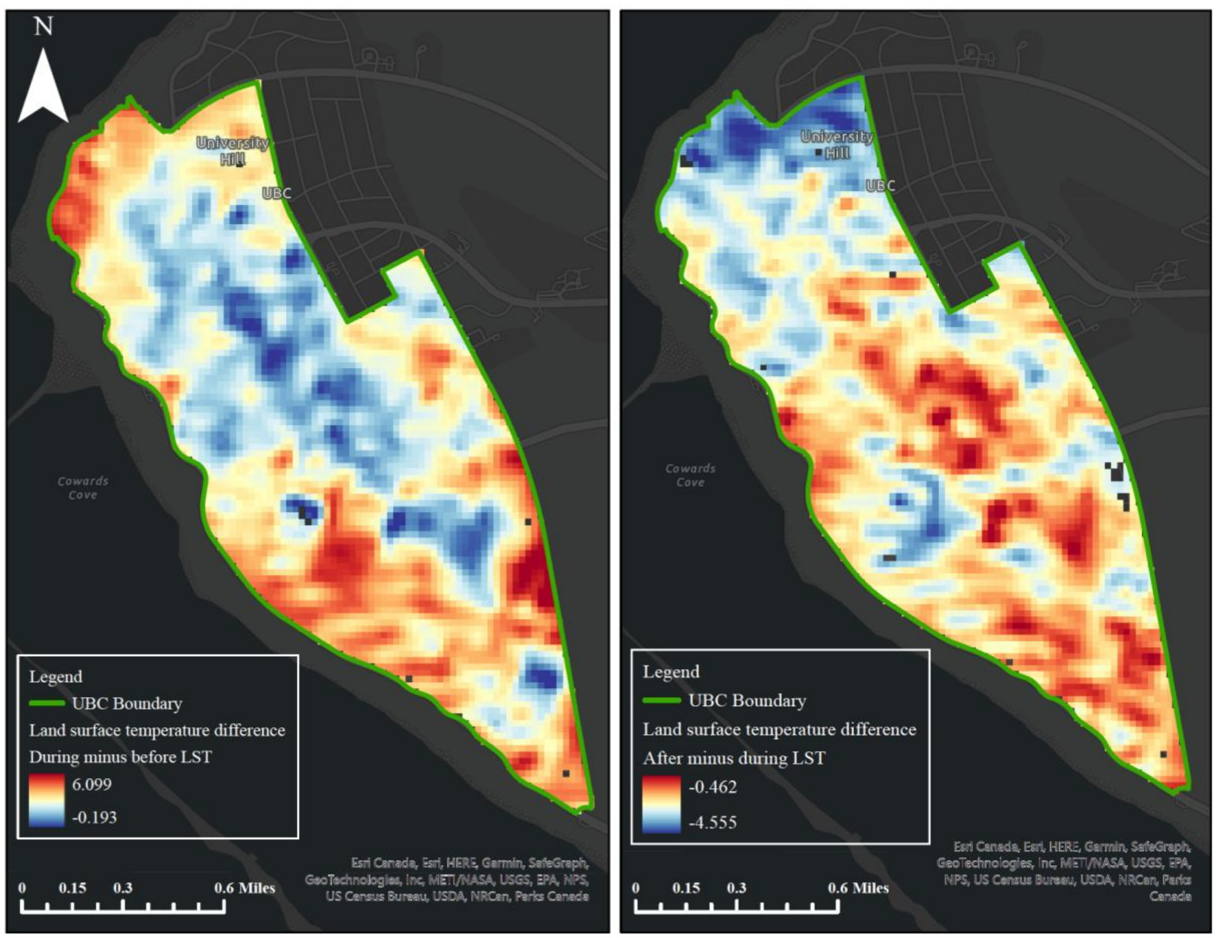

Figure 5. Spatial distribution of ΔLST between before and during (left), as well as, between during and after (right) the Heat Wave on the UBCV campus. The bases map was projected in NAD 1983 UTM Zone 10N and sourced from ESRI.

4.2 Tree Stand Composition

The UBCV campus was dominated by the deciduous stand composition (Figure 6). Coniferous and mixed wood stand compositions were mainly distributed in the northwest corner of the UBCV campus. By comparing the tree stand composition with two ΔLSTs at the Nitobe Memorial Garden and UBC Chemistry Building (Figure 7), there was a higher ΔLST at Nitobe Memorial Garden for both time points than ΔLST at UBC Chemistry Building.

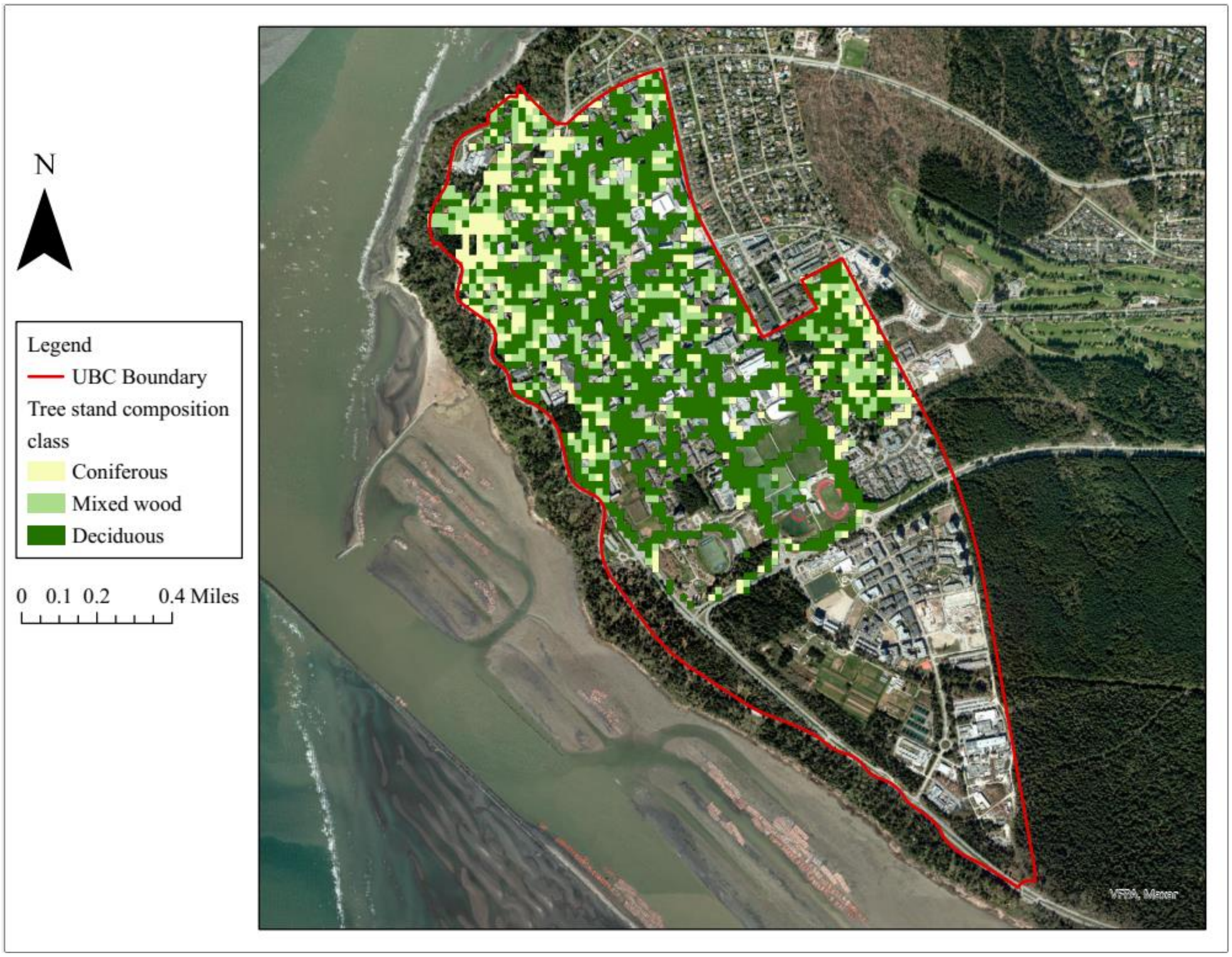

Figure 6. Classification map of tree stand compositions at the UBCV campus in the following classification scheme: coniferous, deciduous, and mixed wood stand compositions. The bases map was projected in NAD1983 UTM Zone 10N and sourced from ESRI.

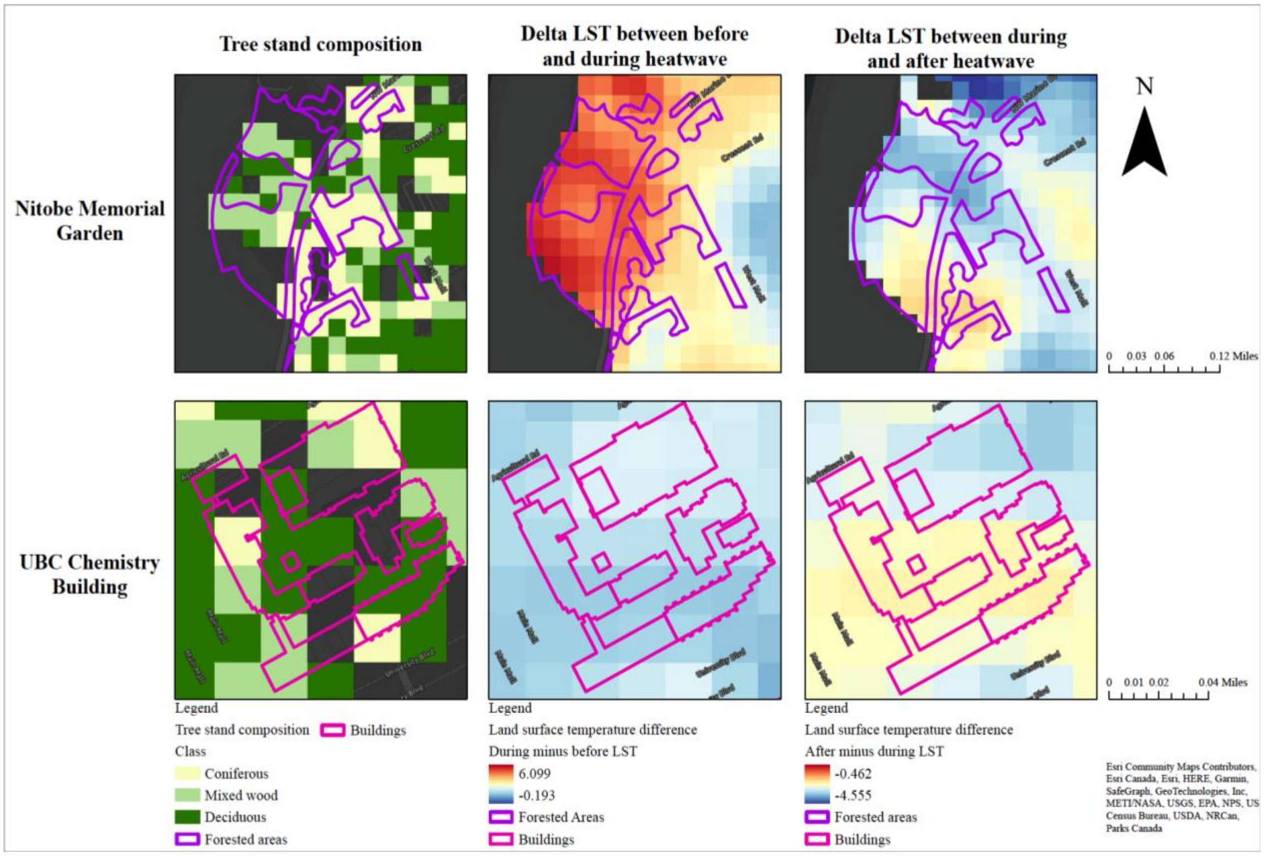

Figure 7. Comparison of the tree stand composition and ΔLST at two different time points (before ~ during, and during ~ after) at the Nitobe Memorial Garden and UBC Chemistry Building. The base map was projected in NAD1983 UTM Zone 10N and sourced from ESRI.

4.3 Relationship between LST Differences and Tree Stand Composition

To quantify the relationship between ΔLST and tree stand composition at two different time points, a boxplot of ΔLST for three tree stand compositions was reported in Figure 8. Between before and during the heatwave (Figure 8, red), LST increased and the majority of ΔLST were positive. However, ΔLST were all negative and LST decreased between during and after the heatwave (Figure 8, blue). Additionally, the interquartile ranges and mean partially overlapped among deciduous, coniferous, and mixed wood stand compositions. Therefore, Figure 8 showed unclear differences among the three stand components in altering LST. However, Table 5 demonstrated that at least one pair of tree stand compositions differed in mean ΔLST since the p-value (4.445e-06) was smaller than α (0.05).

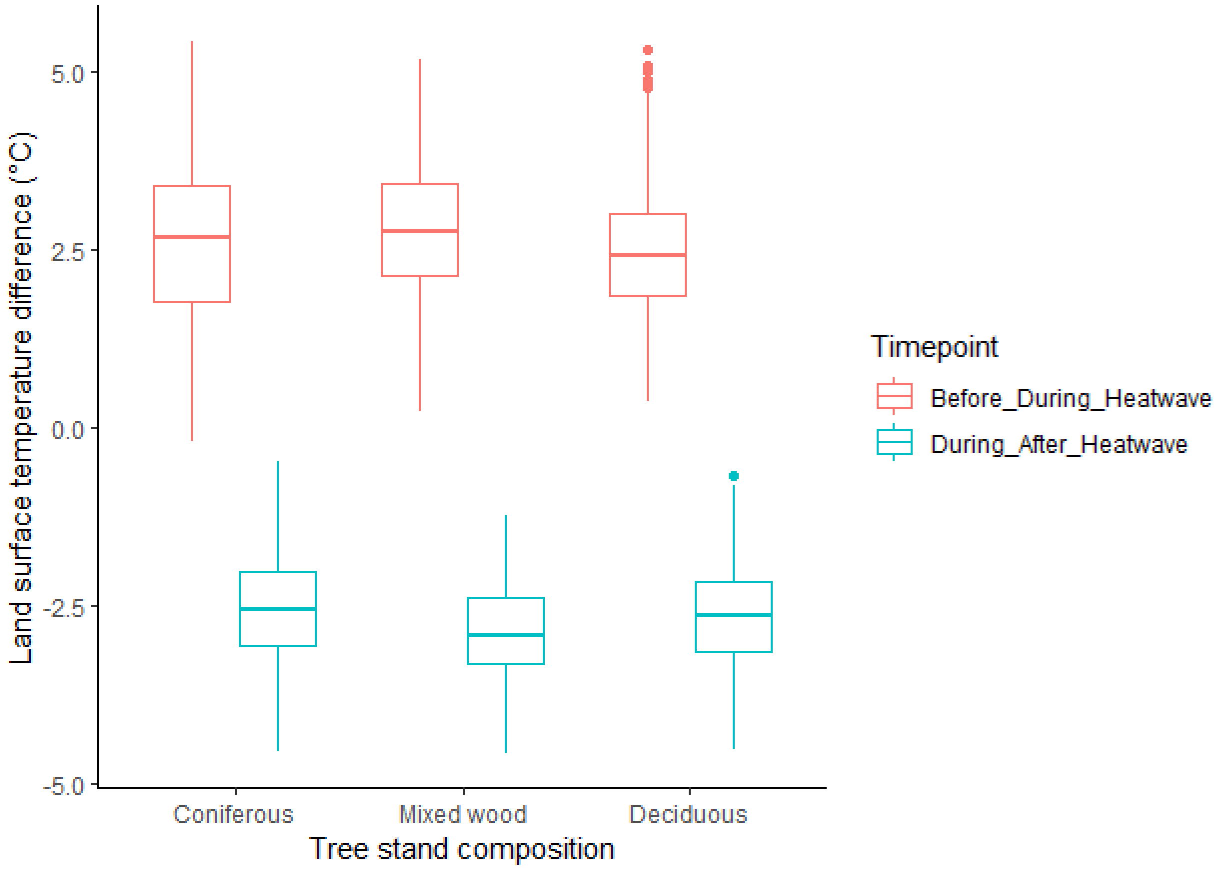

Figure 8. Boxplots of land surface temperature differences (ΔLST, °C) for coniferous, mixed wood, and deciduous stand compositions, colored by the time point.

Table 5. Overview of the ANOVA table generated by the linear mixed effects model.

	F value	**P value**
grp.f	12.347	4.445e-06 ***

To further examine differences in altering LST between pairs of three tree stand compositions, the adjusted p-value of each pair of tree stand compositions was presented in Table 6. Only the p-value of the pair of deciduous and coniferous stand compositions (<.0001) was less than α (0.05), indicating there was a significant difference between ΔLST of deciduous and coniferous stand compositions, while there was no significant difference between ΔLST of other pair of tree stand compositions.

Table 6. Overview of the t-tests' result between pairs of tree stand compositions.

Pairs of tree stand composition	P value
Deciduous - Coniferous	<.0001
Deciduous - Mixed wood	0.1519
Coniferous - Mixed wood	0.8248

To determine the optimal tree stand composition that most effectively mitigates ΔLST throughout the Heat Wave, the estimated coefficients for each tree stand composition were shown in Table 7, representing the effect of tree stand composition on ΔLST. The estimated coefficients of deciduous, coniferous, and mixed wood stand composition were -0.101, 0.124, and 0.081, respectively. Namely, deciduous stand composition was negatively associated with ΔLST, while coniferous and mixed wood stand compositions were positively associated with ΔLST. Additionally, the mean ΔLST of deciduous, coniferous, and mixed wood stand compositions were -0.101, 0.023, and -0.0202, respectively. The mean ΔLST of coniferous stand composition was also significantly different from the mean for deciduous stand composition, because the p value of coniferous stand composition (6.93e-07) was smaller than α (0.05).

Table 7. Overview of the summary table generated by the linear mixed effects model, including estimated coefficient and p value for each tree stand composition.

	Estimate	P value
(Intercept)	-0.10109	0.9751
grp.fConiferous	0.12405	6.93e-07 ***
grp.fMixed wood	0.08088	0.0506

5. Discussion

This study investigated the cooling effect of three tree stand compositions on LST on the UBCV campus during the Heat Wave. It also provided information on the spatial patterns of ΔLST and tree stand compositions, and the relationship between ΔLST and tree stand compositions at two different time points: (1) before ~ during, and (2) during ~ after. The results given in this study demonstrated that tree stand compositions had an impact on altering LST, in particular, deciduous stand compositions had the best urban cooling effectiveness throughout the Heat Wave. In addition, the deciduous stand composition dominated the UBCV campus, and the spatial patterns of two ΔLSTs were consistent during the Heat Wave.

5.1 Spatial Variation of LST and Tree Stand Compositions

According to the spatial patterns of ΔLST and tree stand compositions throughout the Heat Wave, the center of the UBCV campus was dominated by deciduous stand composition with low ΔLST. However, coniferous stand composition was mainly distributed at the edge of the campus, where ΔLST was higher. This trend was consistent at both time points, indicating that changes in LST were related to the type of land cover and tree stand composition.

In the center of the UBCV campus, large academic areas limit the coverage of green space, resulting in concrete structures (e.g., buildings) and impervious surfaces (e.g., build-up lands) taking up most of the area, thus the increase in LST is higher. Oppositely, the UBCV campus is surrounded by densely forested areas, causing areas at the edge of the campus to show a better performance in reducing LST. This is likely because forested areas can mitigate LST through transpiration and evaporation, whereas built-up areas absorb most of the thermal radiation energy to heat the land surface (Zuo et al., 2018). These findings are consistent with other studies, LST is positively correlated with the density of the built-up area, but negatively correlated with the density of the forested area (Estoque et al., 2017; Naeem et al., 2018). Aminipouri et al. (2019) also found that LST can be significantly reduced during extreme hot weather with increased street tree cover in Vancouver. Therefore, LST can be decreased by increasing the forested areas or decreasing the built-up areas. These findings could inform UBC campus planners to develop new urban forest management strategies to improve campus climate resilience.

5.2 Impact of Tree Stand Composition on LST

Deciduous stand composition had the best urban cooling effectiveness. The effect of deciduous and coniferous stand compositions on ΔLST was significantly different, specifically, coniferous stand composition was positively correlated with ΔLST, and deciduous stand composition was negatively correlated with ΔLST throughout the Heat Wave. It is because LST is associated with albedo, where tree species with a higher albedo are generally cooler (Eyster & Beckage, 2022). The cooling effect of forested areas can vary by four times from species to species due to differences in transpiration rates. Deciduous trees have higher near-infrared reflectance and albedo than others, resulting in lower evaporation and transpiration rates, and therefore the greatest cooling effectiveness (Schwaab et al., 2020). These results are similar to the findings presented by Schwaab et al. (2020), deciduous trees (broad-leaved tree species) can locally reduce LST more significantly in summer compared to coniferous trees (needle-leaved species). Zhao et al. (2020) also demonstrated that deciduous trees were more effective at reducing LST than coniferous trees because deciduous trees generally have greater canopy volume. However, Estep & Beckage (2022) proposed a different result that coniferous trees performed substantially better than deciduous trees in reducing urban heat waves in downtown Vancouver during the summer of 2021. This may be because conifers in downtown Vancouver are generally native species that are better adapted to wet temperate rainforest conditions than non-native deciduous trees. Thus, deciduous stand composition showed the best climate resilience during the extreme hot weather, which could enhance the understanding of how the composition of urban forests affects the cooling effectiveness on a finer scale.

5.3 Limitations

The results of this study are likely to be limited by several factors, including data sources, model validation, and lack of independent variables. As the campus tree data is incomplete and only contains data for the academic core of campus, the results may not be representative of the larger area due to the differences in the characteristics or scale of the area. Additionally, it is essential to conduct model validation to ensure the accuracy and reliability of the model, while identifying any errors in the model. However, model validation was not performed in this study because field measurements were not collected. This may lead to bias in the model's predictions and recommendations. Another limitation of this study was that multiple independent variables were not considered, such as the percent cover of buildings and canopy. This may cause over-simplification or inadequate representation of the underlying relationships between LST and tree stand compositions.

5.4 Conclusion and Recommendations

In conclusion, increasing the forested areas, especially the percent cover of deciduous trees, is one of the best options for urban planners to reduce LST. The reduction of LST during extreme hot weather is also critical to mitigating UHI effects on urban landscapes and the negative impacts of hot temperatures on human mental and physical health (Zhao et al., 2020; Zhou et al., 2019). However, urbanization and climate change are expected to continue to increase globally, causing the intensification of UHI effects (Jiao et al., 2017). This could further exacerbate stress on urban green infrastructure. Considering the thermal comfort level of the public and urban biodiversity, mitigation of UHI effects is urgent. Thus, increasing deciduous trees in urban areas is an important strategy in landscape design and urban planning, to improve the urban living environment and enhance the adaptation of urban forests to climate change.

Currently, the efforts of existing campus planning projects to reduce the impact of UHI effect are obvious to all. Climate Action Plan 2030 (CAP 2030) proposes shading, cooling and thermal comfort as three new focuses for improving cooling effects of campus trees, to accelerate the goal of achieving greenhouse gas reductions over the next 15 years on the UBCV campus (Climate Action Plan 2030, n.d.). In response to CAP 2030, I recommend that campus planners consider planting more deciduous trees, while designing more deciduous stand composition on the UBCV campus.

To enhance the accuracy of the model used in this study, I recommend extrapolating the campus tree data by performing a canopy height model, as well as conducting the model validation to calculate residual for each observation and evaluate the accuracy of the model. To improve the performance of the model, the transpiration rate of tree species, percent of canopy cover, and surface roughness of canopy could be added to the model to further assess the transpiration responses of different tree stand compositions on the urban cooling effect. It is crucial to consider multiple independent variables to improve the correlations between the independent variables and LST. Although this study needs several improvement, the findings obtained can still contribute to the development of urban forest management and campus climate protocols to improve resilient and climate-adapted ecosystems on the UBCV campus.

6. References

Aminipouri, M., Knudby, A. J., Krayenhoff, E. S., Zickfeld, K., & Middel, A. (2019). Modelling the impact of increased street tree cover on mean radiant temperature across Vancouver's local climate zones. *Urban Forestry & Urban Greening, 39*, 9-17. https://doi.org/10.1016/j.ufug.2019.01.016

BEC WEB. (n.d.). Retrieved October 29, 2022, from https://www.for.gov.bc.ca/hre/becweb/index.html

Campus Version 2050. (n.d.). Retrieved October 15, 2022, from https://campusvision2050.ubc.ca/

Climate Action Plan 2030 (n.d.). Retrieved September 17, 2022, from https://planning.ubc.ca/cap2030

Cotlier, G. I., & Jimenez, J. C. (2022). The extreme heat wave over western north america in 2021: An assessment by means of land surface temperature. *Remote Sensing (Basel, Switzerland), 14*(3), 561. https://doi.org/10.3390/rs14030561

Devisscher, T., & Almas, A. (2020, May 31). Campus Urban Forest Inventory and Assessment : Phase 1B [R]. doi:http://dx.doi.org/10.14288/1.0392748

Earth Explorer. (n.d.). U.S. Geological Survey. Retrieved October 15, 2022, from https://earthexplorer.usgs.gov

Esri Inc. (2022). Retrieved October 15, 2022, from https://www.esri.com/en-us/arcgis/products/arcgis-pro/overview

Eyster, H. N., & Beckage, B. (2022). Conifers may ameliorate urban heat waves better than broadleaf trees: Evidence from Vancouver, Canada. *Atmosphere, 13*(5), 830. https://doi.org/10.3390/atmos13050830

GIS-Blog. (n.d.). Calculation of Land Surface Temperature (LST) from Landsat 8 using R. Retrieved November 6, 2022, from https://www.gis-blog.com/calculation-of-land-surface-temperature-lst-from-landsat-8-using-r/

Gülçin, D., & van den Bosch, Cecil C. Konijnendijk. (2021). Assessment of above-ground carbon storage by urban trees using LiDAR data: The case of a university campus. *Forests*, *12*(1), 62. https://doi.org/10.3390/f12010062

Hou, H., & Estoque, R. C. (2020). Detecting cooling effect of landscape from composition and configuration: An urban heat island study on hangzhou. *Urban Forestry & Urban Greening, 53*, 126719. https://doi.org/10.1016/j.ufug.2020.126719

Jesus, J. B. D., & Santana, I. D. M. (2017). Estimation of land surface temperature in caatinga area using landsat 8 data. *Journal of Hyperspectral Remote Sensing, 7*(3), 150. https://doi.org/10.29150/jhrs.v7.3.p150-157

Jiao, M., Zhou, W., Zheng, Z., Wang, J., & Qian, Y. (2017). Patch size of trees affects its cooling effectiveness: A perspective from shading and transpiration processes. *Agricultural and Forest Meteorology, 247*, 293-299. https://doi.org/10.1016/j.agrformet.2017.08.013

Lenhardt, H. X. (n.d.). Clean up your Landsat imagery: Removing cloud and cloud shadow. *ArcGIS Blog*. Retrieved November 6, 2022, from https://www.esri.com/arcgis-blog/products/arcgis-pro/imagery/clean-up-your-landsat-imagery-removing-cloud-and-cloud-shadow/

Naeem, S., Cao, C., Qazi, W. A., Zamani, M., Wei, C., Acharya, B. K., & Rehman, A. U. (2018). Studying the association between green space characteristics and land surface temperature for sustainable urban environments: An analysis of Beijing and Islamabad.

ISPRS International Journal of Geo-Information, 7(2), 38. https://doi.org/10.3390/ijgi7020038

Richter, R., Hutengs, C., Wirth, C., Bannehr, L., & Vohland, M. (2021). Detecting tree species effects on forest canopy temperatures with thermal remote sensing: The role of spatial resolution. *Remote Sensing (Basel, Switzerland), 13*(1), 135. https://doi.org/10.3390/rs13010135

Rosado, R. M. G., Guzmán, E. M. A., Lopez, C. J. E., Molina, W. M., García, H. L. C., & Yedra, E. L. (2020). Mapping the LST (land surface temperature) with satellite information and software ArcGis. *IOP Conference Series, 811*(1), 12045. https://doi.org/10.1088/1757-899X/811/1/012045

RStudio Team (2020). RStudio: Integrated Development Environment for R. Boston, MA. Retrieved October 29, 2022, from http://www.rstudio.com/

Schwaab, J., Davin, E. L., Bebi, P., Duguay-Tetzlaff, A., Waser, L. T., Haeni, M., & Meier, R. (2020). Increasing the broad-leaved tree fraction in European forests mitigates hot temperature extremes. *Scientific Reports, 10*(1), 14153. https://doi.org/10.1038/s41598-020-71055-1

Stewart, R. E., Betancourt, D., Davies, J. B., Harford, D., Klein, Y., Lannigan, R., Mortsch, L., O'Connell, E., Tang, K., & Whitfield, P. H. (2017). A multi-perspective examination of heat waves affecting metro vancouver: Now into the future. *Natural Hazards (Dordrecht), 87*(2), 791-815. https://doi.org/10.1007/s11069-017-2793-7

Sutherland, I. (2012). UBC's urban tree canopy: Growing towards sustainability or a declining resource?https://sustain.ubc.ca/sites/sustain.ubc.ca/files/seedslibrary/tree%20canopy%20study%20final_UP.pdf

The University of British Columbia Campus and Community Planning. (2013). University of British Columbia Vancouver Campus. *Campus and Community Planning data*. Retrieved October 29, 2022, from https://hdl.handle.net/11272.1/AB2/ETO8IU

UBC Campus & Community Planning. (n.d.). *Vancouver Campus Plan*. Retrieved October 29, 2022, from https://planning.ubc.ca/planning-development/policies-and-plans/campus-land-use-planning/vancouver-campus-plan

UBCGeodata. (n.d.). Retrieved October 29, 2022, from https://github.com/UBCGeodata/ubc-geospatial-opendata

U.S. Geological Survey. (n.d.). Landsat Collection 1 U.S. Analysis Ready Data DFCB. Retrieved November 6, 2022, from https://www.usgs.gov/media/files/landsat-collection-1-us-analysis-ready-data-dfcb

Vancouver Historical Temperature. (n.d.). Amateur Weather Statistics for Vancouver, British Columbia. Retrieved October 29, 2022, from https://vancouver.weatherstats.ca/metrics/temperature.html

Wang, C., Wang, Z., Wang, C., & Myint, S. W. (2019). Environmental cooling provided by urban trees under extreme heat and cold waves in U.S. cities. *Remote Sensing of Environment*, *227*, 28-43. https://doi.org/10.1016/j.rse.2019.03.024

Wang, W., Wang, H., Lu, X., Zhou, W., He, X., Wang, Q., & Wei, C. (2018). Microclimate regulating functions of urban forests in Changchun City (north-east China) and their associations with different factors. *IForest*, *11*, 140–147. https://doi.org/10.3832/ifor2466-010

Zhao, D., Lei, Q., Shi, Y., Wang, M., Chen, S., Shah, K., & Ji, W. (2020). Role of species and planting configuration on transpiration and microclimate for urban trees. *Forests*, *11*(8), 825. https://doi.org/10.3390/f11080825

Zhou, W., Cao, F., & Wang, G. (2019). Effects of spatial pattern of forest vegetation on urban cooling in a compact megacity. *Forests*, *10*(3), 282. https://doi.org/10.3390/f10030282

Zuo, S., Dai, S., Song, X., Xu, C., Liao, Y., Chang, W., Chen, Q., Li, Y., Tang, J., Man, W., & Ren, Y. (2018). Determining the mechanisms that influence the surface temperature of urban forest canopies by combining remote sensing methods, ground observations, and spatial statistical models. *Remote Sensing*, *10*(11), 1814. https://doi.org/10.3390/rs10111814